Brazilian Journal of Veterinary Parasitology
ISSN 1984-2961 (Electronic)
www.cbpv.org.br/rbpv
Braz. J. Vet. Parasitol., Jaboticabal, v. 28, n. 1, p. 126-133, jan.-mar. 2019
Doi: https://doi.org/10.1590/S1984-296120180098

Original Article

Antitumoral effects of *Amblyomma sculptum* Berlese saliva in neuroblastoma cell lines involve cytoskeletal deconstruction and cell cycle arrest

Efeito antitumoral da saliva do carrapato *Amblyomma sculptum* Berlese em células de neuroblastoma envolve desconstrução do citoesqueleto e parada do ciclo celular

Thatyanne Gradowski do Nascimento[1]; Priscilla Santos Vieira[2]; Sheron Campos Cogo[1]; Marcela Ferreira Dias-Netipanyj[1]; Nilton de França Junior[1]; Diana Aparecida Dias Câmara[3]; Allan Saj Porcacchia[3]; Ronaldo Zucatelli Mendonça[4]; Andréa Novais Moreno-Amaral[1]; Paulo Luiz de Sá Junior[3]; Simone Michaela Simons[4]; Luciana Zischler[2]; Selene Elifio-Esposito[1]*

[1] Programa de Ciências da Saúde, Pontifícia Universidade Católica do Paraná – PUCPR, Curitiba, PR, Brasil

[2] Escola de Ciências da Vida, Pontifícia Universidade Católica do Paraná – PUCPR, Curitiba, PR, Brasil

[3] Laboratório de Genética, Instituto Butantan, São Paulo, SP, Brasil

[4] Laboratório de Parasitologia, Instituto Butantan, São Paulo, SP, Brasil

Received October 30, 2018
Accepted December 18, 2018

Abstract

The antitumor properties of ticks salivary gland extracts or recombinant proteins have been reported recently, but little is known about the antitumor properties of the secreted components of saliva. The goal of this study was to investigate the *in vitro* effect of the saliva of the hard tick *Amblyomma sculptum* on neuroblastoma cell lines. SK-N-SK, SH-SY5Y, Be(2)-M17, IMR-32, and CHLA-20 cells were susceptible to saliva, with 80% reduction in their viability compared to untreated controls, as demonstrated by the methylene blue assay. Further investigation using CHLA-20 revealed apoptosis, with approximately 30% of annexin-V positive cells, and G0/G1-phase accumulation (>60%) after treatment with saliva. Mitochondrial membrane potential ($\Delta\psi m$) was slightly, but significantly ($p < 0.05$), reduced and the actin cytoskeleton was disarranged, as indicated by fluorescent microscopy. The viability of human fibroblast (HFF-1 cells) used as a non-tumoral control decreased by approximately 40%. However, no alterations in cell cycle progression, morphology, and $\Delta\psi m$ were observed in these cells. The present work provides new perspectives for the characterization of the molecules present in saliva and their antitumor properties.

Keywords: Tick saliva, animal toxin, tumor cell death, pediatric cancer.

Resumo

As propriedades antitumorais de extratos de glândulas salivares de carrapatos ou proteínas recombinantes foram relatadas recentemente, mas pouco se sabe sobre as propriedades antitumorais dos componentes secretados da saliva. O objetivo deste estudo foi investigar o efeito *in vitro* da saliva bruta do carrapato duro *Amblyomma sculptum* sobre as linhagens celulares de neuroblastoma. Células SK-N-SK, SH-SY5Y, Be(2)-M17, IMR-32 e CHLA-20 foram suscetíveis à saliva, com redução de 80% na sua viabilidade em comparação com controles não tratados, como demonstrado pelo ensaio de Azul de Metileno. Investigações posteriores utilizando CHLA-20 revelaram apoptose, com aproximadamente 30% de células positivas para anexina-V, e G0/G1 (> 60%) após tratamento com saliva. O potencial de membrana mitocondrial ($\Delta\psi m$) foi reduzido significativamente ($p < 0,05$), e o citoesqueleto de actina foi desestruturado, como indicado pela microscopia de fluorescência. A viabilidade do fibroblasto humano (células HFF-1), usado como controle não tumoral, diminuiu em aproximadamente 40%. No entanto, não foram observadas alterações na progressão do ciclo celular, morfologia e $\Delta\psi m$ nestas células. O presente trabalho fornece novas perspectivas para a caracterização das moléculas presentes na saliva e suas propriedades antitumorais.

Palavras-chave: Saliva do carrapato, toxina animal, morte celular tumoral, câncer pediátrico.

***Correspondence:** Selene Elifio-Esposito. Pontifícia Universidade Católica do Paraná, Rua Imaculada Conceição, 1155, CEP 80215-901, Curitiba, PR, Brasil. e-mail: seleneesposito@gmail.com

Introduction

Ticks are specialized hematophagous ectoparasites of significant medical and public health importance (RANDOLPH, 2009). During the penetration process of the host skin, ticks succeed in blood feeding by manipulating the host's hemostatic, inflammatory, and immune defense mechanisms, due to numerous active components with pharmacological applications (CABEZAS-CRUZ & VALDÉS, 2014; RADULOVIC et al., 2014; STIBRANIOVA et al., 2013). As a source of anti-neoplasic compounds, it has been reported that tick saliva constituents can affect cancer cell proliferation (KAZIMIROVA et al., 2006), apoptosis (AKAGI et al., 2012), migration and invasion (POOLE et al., 2013), and tumor growth and angiogenesis (CARNEIRO-LOBO et al., 2009). Specifically, the cytotoxicity of *Amblyomma sculptum* Berlese crude saliva (CS) has been demonstrated in melanoma, pancreatic adenocarcinoma (SIMONS et al., 2011), and breast cancer cells (SOUSA et al., 2018). Interestingly, no cytotoxicity was observed in human fibroblasts or non-neoplastic mammary gland cell lines.

Neuroblastoma (NB) is the most common extracranial solid pediatric tumor. These tumors, which account for 15% of pediatric cancer deaths, occur preferentially in young children with a median age at diagnosis of 18 months (KAMIHARA et al., 2017). In the last 30 years, although significant progress has been achieved in the treatment for high-risk NB, the long-term survival for this group of patients remains under 50%, emphasizing the need for more effective treatments (PINTO et al., 2015).

Despite the advances in the transcriptomic and proteomic characterization of tick´s salivary proteins, the biological functions of most of these proteins and their potential for therapeutic and biotechnological use remain unknown (FRANCISCHETTI et al., 2010). Therefore, the search for molecules with antitumor potential in the secreted saliva of ticks may reveal new components of high therapeutic value. In the present study, we demonstrated that the CS of *A. sculptum* shows a high *in vitro* cytotoxic and anti-proliferative effect in NB cells that involves reduction of the mitochondrial membrane potential ($\Delta\psi m$) and rearrangement of the cytoskeleton.

Material and Methods

Saliva collection

To obtain saliva, 125 female and 50 male ticks were fed the blood of domestic rabbits (*Oryctolagus cuniculus*) without prior tick infestations. Male (10) and female (25) ticks were placed inside a cotton chamber (10 cm x 15 cm) on the back of the rabbits. Females that reached 1.0 cm in width and 1.2 cm in length on the eighth day of feeding were removed by torsion from the rabbits' backs. Salivation was induced using the methodology described by Kaufman (1978) with minor modifications. Briefly, ticks were ventrally attached to a double-sided tape on a wood base, and 5 µl to 10 µl of a dopamine solution (Sigma-Aldrich, St. Louis, MO, USA; 5% w/v in 0.15 M NaCl) were injected into the dorsal region using a micrometric syringe. Saliva was collected for 4 h at room temperature in microcapillary tubes fastened to the wood base, with one end in contact with the female's hypostome. The collected saliva was immediately frozen on dry ice. Saliva samples were pooled, filtered (0.22 µm), aliquoted, frozen on dry ice and ethanol, and kept at -80 °C until use. All experiments were carried out using protocols approved by the Ethics Committee for the Use of Animals of the Butantan Institute (CEUA No 1872100317). CS protein concentration was estimated using the Bradford protein assay (BRADFORD, 1976).

Cell culture

Human NB cells (Be(2)-M17, CHLA-20, IMR-32, SK-N-SH, and SH-SY5Y) and human foreskin fibroblasts (HFF-1) were cultivated in Dulbecco's Modified Eagle Medium (DMEM)/Ham's F-12 medium (LGC Biotechnology, São Paulo, Brazil) supplemented with 10% heat inactivated fetal bovine serum (FBS), 100 IU/mL penicillin, and 0.1 mg/mL streptomycin (all from Gibco, Thermo Fisher Scientific, Waltham, MA, USA). Cells were maintained at 37 °C in 5% CO_2. CHLA-20 and IMR-32 NB cells were kindly gifted by St. Jude Children's Hospital (Memphis, TN, USA), SK-N-SH, Be(2)-M17, and SH-SY5Y were obtained from the American Type Culture Collection (ATCC, Manassas, VA, USA). HFF-1 was obtained from the Rio de Janeiro Cell Bank, RJ, Brazil.

Viability assay

Cells were seeded in 96-well plates (1×10^4 cells/well) and incubated with different concentrations of saliva (serial dilution of CS from 20 µg protein/mL) for 24, 48, and 72 h. Cells were fixed with methanol and stained with aqueous methylene blue solution (0.05% w/v) for 10 min. Repeated washings were performed to remove any excess stain that could interfere with reading. After drying, 0.1 M HCl was added, and the plate was read on a VersaMax ™ ELISA Microplate Reader (Molecular Devices, San Jose, CA, USA) at 630 nm wavelength.

Clonogenic Assay

Be(2)-M17, CHLA-20, SK-N-SH, SH-SY5Y, and HFF-1 cells were seeded in 24-well plates (1×10^5 cells/well), and treated with 5.0 µg/mL, 10.0 µg/mL, and 20.0 µg/mL CS for 72 h. Cells (1×10^2 cells/well) were transferred to a 24-well plate and cultured for 21 days. Cells were then washed, fixed in methanol, and stained with 0.05% crystal violet solution.

Fluorescence microscopy

CHLA-20, IMR-32, and HFF-1 cells were seeded on sterile glass cover slips in 24-well plates and treated with 20 µg protein/mL CS for 48 h. For fluorescence microscopy, cells were fixed with 3.7% paraformaldehyde and permeabilized by 0.02% Triton X-100 diluted in phosphate buffered saline (PBS) containing 10% FBS for 5 min. To stain actin filaments, cells were labeled with phalloidin-FITC (Molecular Probes, Invitrogen, Carlsbad, CA, USA) in a buffer containing 0.01% Triton X-100 and

1 mg/mL RNase diluted in PBS. For mitochondrial studies, cells were stained with MitoTracker Red for 45 min under growth conditions. Image analysis was performed with a Nikon Eclipse Ni fluorescence microscope (Tokyo, Japan). Post-acquisition image processing was performed using Image J software (version 14.1, National Institutes of Health, Bethesda, MD, USA).

Flow cytometry detection of apoptosis

CHLA-20 and HFF-1 cells were seeded in 24-well plates (1×10^5 cells/well) following treatment with 20 µg protein/mL CS for 72 h, and stained with Annexin-V and 7-AAD (BD Biosciences, San Jose, CA) according to the manufacturer's instructions. Cells were analyzed by flow cytometry using the BD FACSCalibur instrument (BD Biosciences). Data acquisition and analyses were performed using BD Cell Quest Pro or FlowJo. The measurement of caspase-3 activation was performed using the PE Active Caspase-3 Apoptosis Kit (BD Biosciences). Mitochondrial integrity was evaluated using MitoStatus Red (BD Pharmingen, BD Biosciences).

Cell cycle analysis

CHLA-20 and HFF-1 cells were treated for 48 h with 20 µg protein/mL CS, harvested, fixed in cold 70% ethanol, and stored at -20 °C. For cell cycle analysis, cells were washed twice in PBS and re-suspended in the same solution, followed by incubation at 37 °C for 45 min with 10 mg/mL RNase and 1 mg/mL propidium iodide (Sigma-Aldrich, St. Louis, MO, USA). Flow cytometry analysis was performed using a FACSCalibur system. Cellular DNA content at the different cell cycle phases was determined using ModFit LT software (Verity Software House, Topsham, ME, USA).

Statistical analysis

Statistical analysis was performed using GraphPad Prism software version 7.0 (GraphPad, San Diego, CA, USA). Quantitative data were expressed as mean ± SD, and analyzed by ANOVA, followed by the multiple comparative Dunnett test, or Student *t*-test, when applicable. A significance threshold of $p < 0.05$ was used.

Results

A. sculptum CS decreased the viability of all NB cell lines

The concentration of protein in CS was estimated at 104.2 µg/mL. For assays CS concentration was determined by the content of protein. Methylene blue assay results showed that all of the NB cell lines tested were susceptible to CS (Figure 1A). For most cell lines, loss in cell viability was time- and dose-dependent. IC_{50} values (i.e., the CS concentrations that were cytotoxic for 50% of the cell populations) were calculated using the 72-h incubation curves (Table 1). This analysis showed a similar CS toxicity in all NB cells tested (from 3.0 to 9.2 µg/mL), when compared to the fibroblast cell line HFF-1 (25.7 µg/mL).

Table 1. Comparison of the effect of CS on cell viability.

Cell Line	Viable cells (%)[A] Mean ± SEM	IC50[B] µg/ml
SK-N-SH	26.4 ± 8.2	9.2
SH-SY5Y	17.9 ± 4.8	5.4
Be(2)-M17	11.6 ± 4.8	6.9
CHLA-20	19.1 ± 4.8	3.0
HFF-1	56.5 ± 13.1	25.6

[A] Percentage of viable cells determined after incubation of cell lines for 72 h with 20 µg/mL protein equalized CS; [B] IC50 of CS calculated using the 72 h incubation curves.

Tumor cells also exhibited significant morphological changes upon exposure to CS, such as loss of elongated shape, which is characteristic of neuroblasts (as was observed in the untreated cells) (Figure 1B). However, SH-SY5Y cells maintained an elongated shape, but lost cellular aggregation as compared to the untreated control (Figure 1B). Clonogenic assay results, as shown in Figure 1C, indicate that colony formation was reduced with higher concentrations of CS, notably for the Be(2)-M17 cell line. However, except for these cells, NB cells recovered clonogenic capability in the absence of CS.

A. sculptum CS induced cytoskeleton disassembly

The fluorescence micrographs in Figure 2 illustrate the morphological changes in CHLA-20 and IMR-32 NB cell lines after treatment with 20 µg/mL CS for 48 h, as evidenced by phalloidin staining. Rounding of the cells and loss of cellular interactions were detected, suggesting a deconstructive effect of the treatment on the actin filaments in cells. In addition, MitoTracker staining was significantly reduced in IMR-32 cells after treatment with CS, which indicates a strong reduction in mitochondrial activity. No difference in mitochondrial activity was observed in the CHLA-20 cells. No significant morphologic alterations in the fluorescence pattern of HFF-1 cells were observed after exposure to CS.

A. sculptum CS induced apoptosis and cell cycle arrest in NB cells

The dot-blot analysis shown in Figure 3B demonstrates that the remaining NB cells shifted towards Q2 (double marked cells) after treatment with 20 µg/mL CS (48 h), which corresponds to 30% of apoptotic cells (Figure 2C). In fibroblasts, although a high apoptotic index was found in the untreated cells (approximately 15%), it did not increase further after CS treatment. The ability of CS to alter the function of mitochondria in CHLA-20 cells was investigated by flow cytometry. Cells treated with CS exhibited a small, but significant, decrease in MitoStatus Red fluorescence intensity, after 24 h incubation (Figure 3D, shift to G1). Even with a reduced number of cells exposed to CS after 48 and 72 h, the remaining cells did not show reduced mitochondrial activity when

compared with the untreated cells. Flow cytometric analysis of DNA content confirmed high sensitivity of the NB cell lines in comparison to the fibroblast cells. CS treatment exerted a pro-apoptotic effect (evidenced by the presence of a sub-G0/G1 peak) accompanied by cell cycle arrest at G1 in the CHLA-20 cells (Figure 4). CS treatment did not affect the cell cycle course of the HFF-1 cells.

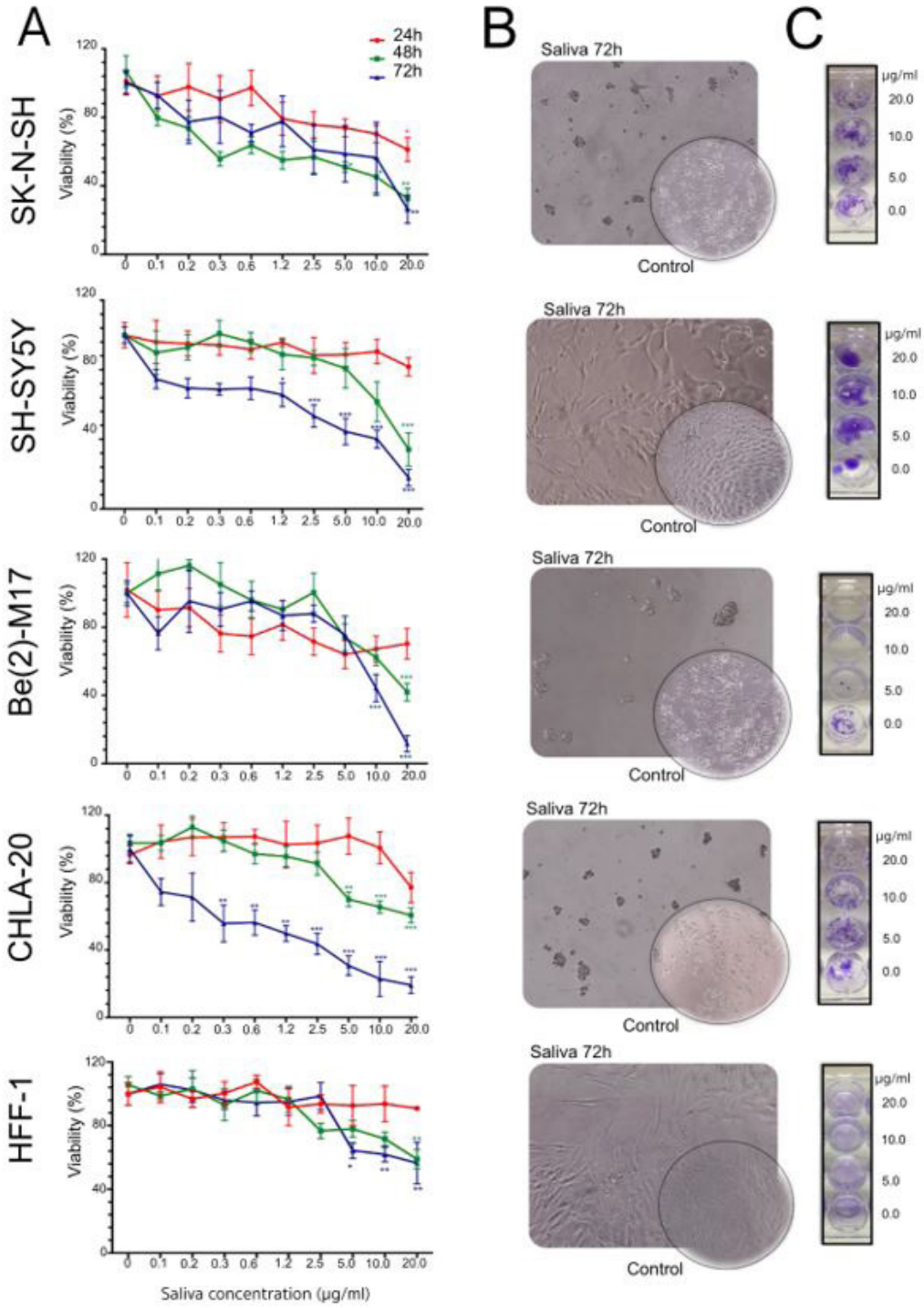

Figure 1. Tick crude saliva (CS) induces cell death in different NB tumor cell lines. NB cells and human foreskin fibroblasts (HFF-1) were treated with 20 µg/mL CS for 48 h. A) Cell viability was determined by the methylene blue assay performed in three independent tests. Data were analyzed using two-way ANOVA followed by Dunnett´s multiple comparison test, in which each group mean was compared with the mean of untreated control. Significant differences are indicated as (*) $p < 0.05$, (**) $p < 0.01$ and (***) $p < 0.001$. B) Light microscopy of cell culture after 72 h incubation with 20 µg/mL CS. C) Representative results of clonogenic assays after independent assays were performed in triplicate.

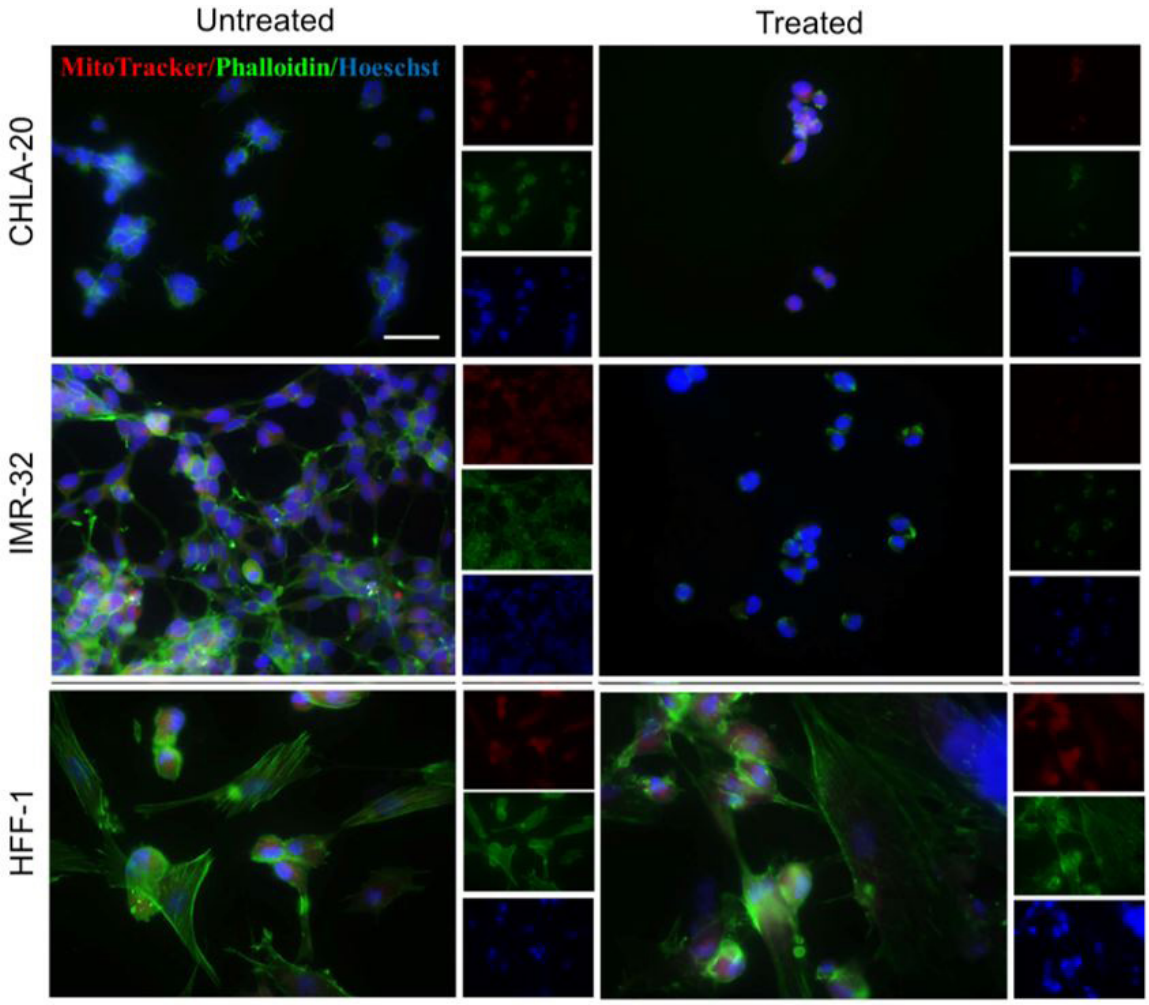

Figure 2. Mitochondria and F-actin disposal detection. Tumor and fibroblast cells were treated for 48 h with CS and stained with MitoTracker (red), phalloidin-FITC (green) and DAPI (blue). The slides were mounted and observed under fluorescent microscopy at 400× magnification. The experiment was performed in triplicate, and the data shown are representative of each cell line tested.

Discussion

CS from hematophagous arthropod vectors mediates the successful withdrawal of blood from their hosts by interacting and modifying the functions of a diverse array of cells in the host tissues. In this study, we found that the CS of *A. sculptum*, (previously cited as *Amblyomma cajennense*; NAVA et al., 2014), exhibited cytotoxic effects on different human NB cells, supporting the antitumor potential of CS, as reported by Sousa et al. (2015).

Clinical heterogeneity is one of the hallmarks of neuroblastomas (WALTON et al., 2004). NB cell lines can be used as surrogates of NB tumor phenotypes and reveal *in vitro* their sensitivity to therapeutic compounds. In this study, we initially investigated whether CS could specifically affect undifferentiated NB cells. The SK-N-SH cell line is highly heterogeneous, composed of both of differentiated NB cells (N-type and S-type), and the more tumorigenic undifferentiated I-type cells (BOEVA et al., 2017; ROSS et al., 2015; WALTON et al., 2004). The SH-SY5Y line is a subclone of the SK-N-SH line (THIELE, 1998), and consists of a mixture of the three cell types, along with differentiated N-cells. On the other hand, the Be(2)-M17 and IMR-32 NB cell lines present a fully differentiated phenotypic profile. Our analysis of cell viability showed that all NB cells tested were highly sensitive to CS treatment, with non-significant differences in the IC50, despite their distinct phenotypes.

Cells lines established from patients at diagnosis can be more sensitive to cytotoxic agents than those obtained during disease progression (KESHELAVA et al.,1998). High-risk NB treatment regimens include five to six cycles of induction chemotherapy (PINTO et al., 2015), which for some patients can cause the development of a chemotherapy-refractory disease, suggesting the occurrence of an *in vivo* selection of drug-resistant tumor cells. The CHLA-20 cell line, predominantly consisting of differentiated cells, was established from a metastatic tumor after chemotherapy with cisplatin, cyclophosphamide, doxorubicin, and teniposide (KESHELAVA et al., 1998), forming a robust model to evaluate the potential of cytotoxic agents, such as CS, on cells that acquired treatment resistance. Here, we showed that CHLA-20 cells were

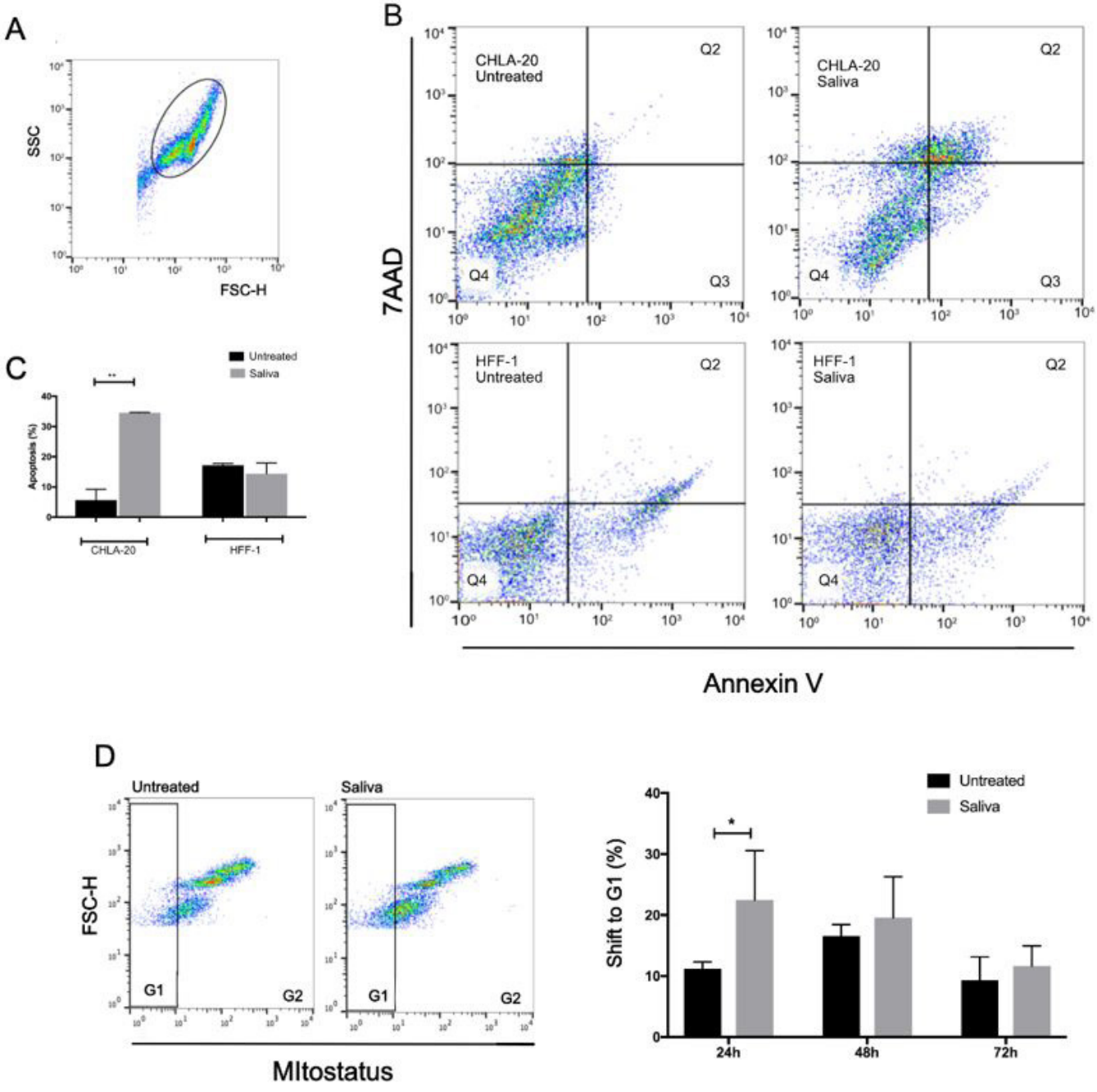

Figure 3. *A. sculptum* CS caused apoptosis and disruption of the mitochondrial membrane potential (ΔmΨ) in NB cells. CHLA-20 and HFF-1 cells were treated with 20 µg/mL CS for 72 h and analyzed by flow cytometry. A) Population of CHLA-20 cells gated and used in the analysis. B) Analysis of apoptosis with Annexin V/7-AAD staining, representative result for CHLA-20 cells. C) Comparative analysis of apoptosis after three independent assays. D) MitoStatus reagent was used to assess mitochondrial membrane potential (Δψm) of CHLA-20 cells. While G1 area represents the cell population with depolarized mitochondria, G2 area shows the live cell population with polarized mitochondria. Results are expressed as mean ± SD, and were analyzed using Student´s *t*-test to compare differences between treated group with untreated control. Statistical significances are indicated as (*) $p < 0.05$ (**) and $p < 0.01$.

very sensitive to CS, as demonstrated by the decrease in the percentage of viable cells after 48 and 72 h incubation, and by the degree of the fractional DNA as a sub G0/G1 population, indicating cell death, as observed in the cell cycle assay.

Additionally, incubation of CHLA-20 cells with CS led to the activation of apoptosis. Approximately 30% of the treated cells exhibited phosphatidylserine (PS) on the outer layer of the plasma membrane, along with reduction in the mitochondrial membrane

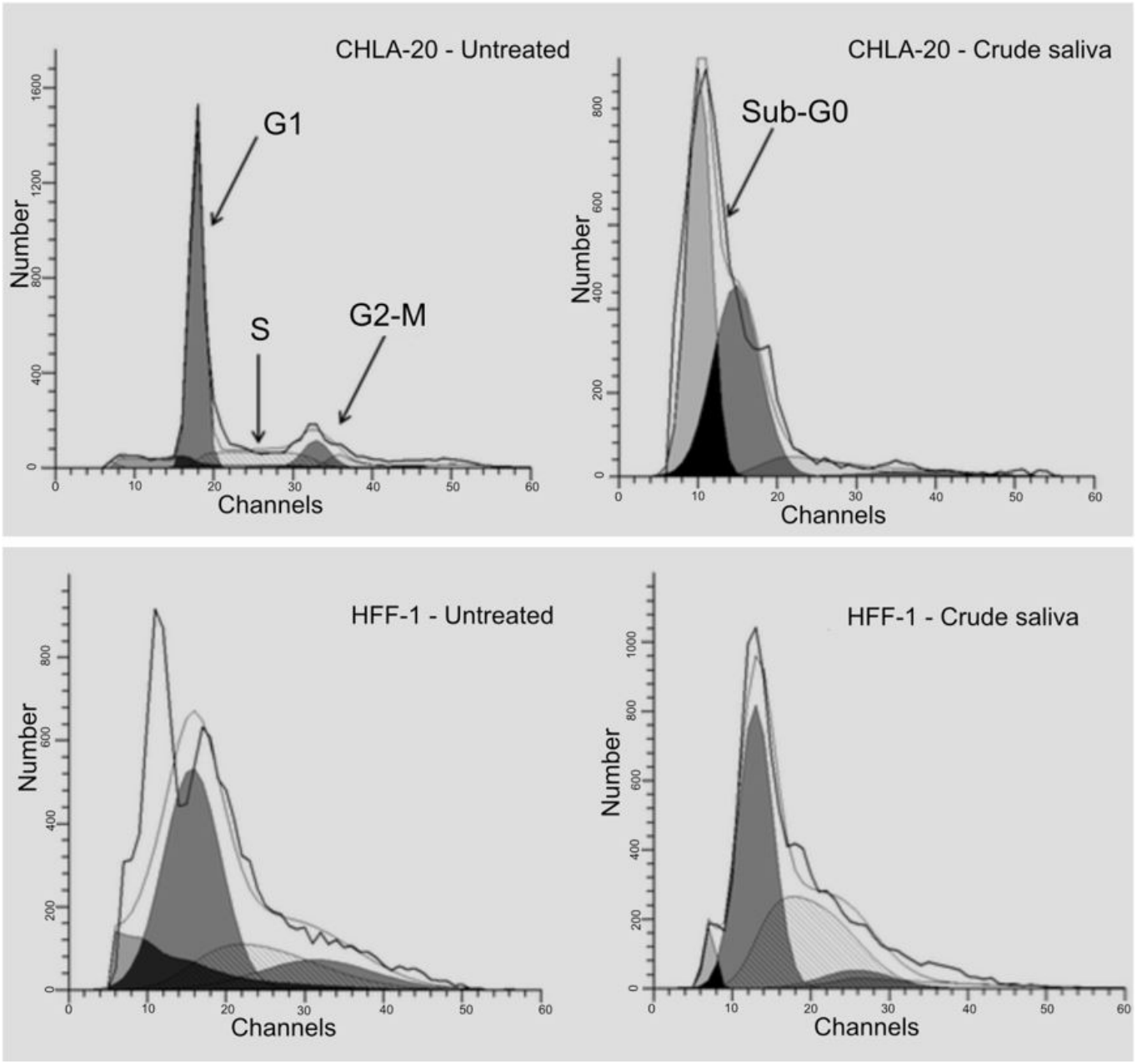

Figure 4. Effects of *A. sculptum* CS on cell cycle progression. Representative histograms of cell cycle analysis of the CHLA-20 and HFF-1 cells after exposure to CS for 48 h.

potential (at 24h incubation), indicating that apoptosis may not be the primary effect of CS on these cells. We further observed that CS did not induce caspase-3 activation (data not shown) in CHLA-20 cells. On the other hand, cytoskeleton disruption was highly apparent in both CHLA-20 and IMR-32 cells, suggesting that detachment of cells, regardless of apoptosis activation, is a determinant for the loss of cell viability and cell death induced by CS treatment.

A previous study demonstrated that the secreted saliva of the hard tick *Ixodes scapularis* Say was a potent inhibitor of angiogenesis and microvascular endothelial cell proliferation (FRANCISCHETTI et al., 2005). This effect was further accompanied by a change in cell shape (shrinkage of the cytoplasm with loss of cell-cell interactions) and activation of apoptosis, which appeared to be mediated by the endothelial cell α5β1 integrin. We found similar morphological alterations in NB cell monolayers; however, we did not investigate the involvement of integrins.

The process of cell death triggered by cytotoxic agents is heterogeneous and complex, and although our results indicate that CS cytotoxicity led to apoptotic activation in NB cell lines, other mechanisms of cell death could be involved.

In summary, our study demonstrated that *A. sculptum* CS possesses compounds that affect proliferation and cytoskeleton architecture of NB tumor cells, with no effect on fibroblasts, supporting its therapeutic antitumor potential. Additional *in vitro* and *in vivo* analyses are required for the identification and

isolation of the active molecules from CS that are responsible for the cell phenotype alterations observed in the NB cells in our study.

Acknowledgements

We thank Dr. Bonald C. Figueiredo from Pelé Pequeno Príncipe Research Institute for the CHLA-20 and IMR-32 neuroblastoma cells kindly gifted. Dr. Luciane R. Cavalli for providing language help and proof reading, and Dr. Lucia de Noronha for comments that greatly improved the manuscript. We wish to express our knowledge for the institutional support of the Butantan Institute and Butantan Foundation for maintenance of the animal facility.

This work was supported by the Coordenação de Aperfeiçoamento de Pessoal de Nível Superior (CAPES-COFECUB 16/2015 #880/2017, Finance Code 001), Fundação Araucária de Apoio ao Desenvolvimento Científico e Tecnológico do Estado do Paraná - Fundação Araucária (FA 09/2016).

References

Akagi EM, Sá PL Jr., Simons SM, Bellini MH, Barreto SA, Chudzinski-Tavassi AM. Pro-apoptotic effects of Amblyomin-X in murine renal cell carcinoma "in vitro". *Biomed Pharmacother* 2012; 66(1): 64-69. http://dx.doi.org/10.1016/j.biopha.2011.11.015. PMid:22281290.

Boeva V, Louis-Brennetot C, Peltier A, Durand S, Pierre-Eugene C, Raynal V, et al. Heterogeneity of neuroblastoma cell identity defined by transcriptional circuitries. *Nat Genet* 2017; 49(9): 1408-1413. http://dx.doi.org/10.1038/ng.3921. PMid:28740262.

Bradford MM. A rapid and sensitive method for the quantitation of microgram quantities of protein utilizing the principle of protein-dye binding. *Anal Biochem* 1976; 72(1-2): 248-254. http://dx.doi.org/10.1016/0003-2697(76)90527-3. PMid:942051.

Cabezas-Cruz A, Valdés JJ. Are ticks venomous animals? *Front Zool* 2014; 11(47): 1-18. http://dx.doi.org/10.1186/1742-9994-11-47. PMid:25006341.

Carneiro-Lobo TC, Konig S, Machado DE, Nasciutti LE, Forni MF, Francischetti IMB, et al. Ixolaris, a tissue factor inhibitor, blocks primary tumor growth and angiogenesis in a glioblastoma model. *J Thromb Haemost* 2009; 7(11): 1855-1864. http://dx.doi.org/10.1111/j.1538-7836.2009.03553.x. PMid:19624457.

Francischetti IM, Calvo E, Andersen JF, Pham VM, Favreau AJ, Barbian KD, et al. Insight into the Sialome of the Bed Bug, *Cimex lectularius*. *J Proteome Res* 2010; 9(8): 3820-3831. http://dx.doi.org/10.1021/pr1000169. PMid:20441151.

Francischetti IM, Mather TN, Ribeiro JM. Tick saliva is a potent inhibitor of endothelial cell proliferation and angiogenesis. *Thromb Haemost* 2005; 94(1): 167-174. PMid:16113800.

Kamihara J, Bourdeaut F, Foulkes WD, Molenaar JJ, Mossé YP, Nakagawara A, et al. Retinoblastoma and neuroblastoma predisposition and surveillance. *Clin Cancer Res* 2017; 23(13): e98-e106. http://dx.doi.org/10.1158/1078-0432.CCR-17-0652. PMid:28674118.

Kaufman WR. Actions of some transmitters and their antagonists on salivary secretion in a tick. *Am J Physiol* 1978; 235(1): R76-R81. PMid:677342.

Kazimírová M, Dovinová I, Rolníková T, Tóthová L, Hunáková L. Anti-proliferative activity and apoptotic effect of tick salivary gland extracts on human HeLa cells. *Neuroendocrinol Lett* 2006; 27(Suppl 2): 48-52. PMid:17159778.

Keshelava N, Seeger RC, Groshen S, Reynolds CP. Drug resistance patterns of human neuroblastoma cell lines derived from patients at different phases of therapy. *Cancer Res* 1998; 58(23): 5396-5405. PMid:9850071.

Nava S, Beati L, Labruna MB, Cáceres AG, Mangold AJ, Guglielmone AA. Reassessment of the taxonomic status of *Amblyomma cajennense* (Fabricius, 1787) with the description of three new species, *Amblyomma tonelliae* n. sp., *Amblyomma interandinum* n. sp. and *Amblyomma patinoi* n. sp., and reinstatement of *Amblyomma mixtum* Koch, 1844, and *Amblyomma sculptum* Berlese, 1888 (Ixodida: Ixodidae). *Ticks Tick Borne Dis* 2014; 5(3): 252-276. http://dx.doi.org/10.1016/j.ttbdis.2013.11.004. PMid:24556273.

Pinto NR, Applebaum MA, Volchenboum SL, Matthay KK, London WB, Ambros PF, et al. Advances in risk classification and treatment strategies for neuroblastoma. *J Clin Oncol* 2015; 33(27): 3008-3017. http://dx.doi.org/10.1200/JCO.2014.59.4648. PMid:26304901.

Poole NM, Nyindodo-Ogari L, Kramer C, Coons LB, Cole JA. Effects of tick saliva on the migratory and invasive activity of Saos-2 osteosarcoma and MDA-MB-231 breast cancer cells. *Ticks Tick Borne Dis* 2013; 4(1-2): 120-127. http://dx.doi.org/10.1016/j.ttbdis.2012.09.003. PMid:23168047.

Radulović ŽM, Kim TK, Porter LM, Sze SH, Lewis L, Mulenga AA. 24-48 h fed *Amblyomma americanum* tick saliva immuno-proteome. *BMC Genomics* 2014; 15(518): 1-30. http://dx.doi.org/10.1186/1471-2164-15-518. PMid:24962723.

Randolph SE. Tick-borne disease systems emerge from the shadows: the beauty lies in molecular detail, the message in epidemiology. *Parasitology* 2009; 136(12): 1403-1413. http://dx.doi.org/10.1017/S0031182009005782. PMid:19366480.

Ross RA, Walton JD, Han D, Guo HF, Cheung NK. A distinct gene expression signature characterizes human neuroblastoma cancer stem cells. *Stem Cell Res* 2015; 15(2): 419-426. http://dx.doi.org/10.1016/j.scr.2015.08.008. PMid:26342562.

Simons SM, Sá PL Jr., Faria F, Batista IF, Barros-Battesti DM, Labruna MB, et al. The action of *Amblyomma cajennense* tick saliva in compounds of the hemostatic system and cytotoxicity in tumor cell lines. *Biomed Pharmacother* 2011; 65(6): 443-450. http://dx.doi.org/10.1016/j.biopha.2011.04.030. PMid:21723081.

Sousa ACP, Oliveira CJF, Szabó MPJ, Silva MJB. Anti-neoplastic activity of *Amblyomma sculptum, Amblyomma parvum* and *Rhipicephalus sanguineus* tick saliva on breast tumor cell lines. *Toxicon* 2018; 148: 165-171. http://dx.doi.org/10.1016/j.toxicon.2018.04.024. PMid:29705147.

Sousa ACP, Szabó MPJ, Oliveira CJF, Silva MJB. Exploring the anti-tumoral effects of tick saliva and derived components. *Toxicon* 2015; 102: 69-73. http://dx.doi.org/10.1016/j.toxicon.2015.06.001. PMid:26079950.

Stibrániová I, Lahová M, Bartíková P. Immunomodulators in tick saliva and their benefits. *Acta Virol* 2013; 57(2): 200-216. http://dx.doi.org/10.4149/av_2013_02_200. PMid:23600877.

Thiele CJ. Neuroblastoma cell lines. In: Masters J. *Human cell culture*. Lancaster: Kluwer Academic Publishers; 1998. (vol. 1) p. 21-53. http://dx.doi.org/10.1007/0-306-46872-7_2.

Walton JD, Kattan DR, Thomas SK, Spengler BA, Guo HF, Biedler JL, et al. Characteristics of stem cells from human neuroblastoma cell lines and in tumors. *Neoplasia* 2004; 6(6): 838-845. http://dx.doi.org/10.1593/neo.04310. PMid:15720811.